

2 **Optimal visual–vestibular integration under conditions**
3 **of conflicting intersensory motion profiles**

4 **John S. Butler · Jennifer L. Campos ·**
5 **Heinrich H. Bühlhoff**

6 Received: 22 May 2014 / Accepted: 20 October 2014
7 © Springer-Verlag Berlin Heidelberg 2014

AQ1 Abstract Passive movement through an environment is typically perceived by integrating information from different sensory signals, including visual and vestibular information. A wealth of previous research in the field of multisensory integration has shown that if different sensory signals are spatially or temporally discrepant, they may not combine in a statistically optimal fashion; however, this has not been well explored for visual–vestibular integration. Self-motion perception involves the integration of various movement parameters including displacement, velocity, acceleration and higher derivatives such as jerk. It is often assumed that the vestibular system is optimized for the processing of acceleration and higher derivatives, while the visual system is specialized to process position and velocity. In order to determine the interactions between different spatiotemporal properties for self-motion perception, in Experiment 1,

we first asked whether the velocity profile of a visual trajectory affects discrimination performance in a heading task. Participants performed a two-interval forced choice heading task while stationary. They were asked to make heading discriminations while the visual stimulus moved at a constant velocity (C-Vis) or with a raised cosine velocity (R-Vis) motion profile. Experiment 2 was designed to assess how the visual and vestibular velocity profiles combined during the same heading task. In this case, participants were seated on a Stewart motion platform and motion information was presented via visual information alone, vestibular information alone or both cues combined. The combined condition consisted of congruent blocks (R-Vis/R-Vest) in which both visual and vestibular cues consisted of a raised cosine velocity profile and incongruent blocks (C-Vis/R-Vest) in which the visual motion profile consisted of a constant velocity motion, while the vestibular motion consisted of a raised cosine velocity profile. Results from both Experiments 1 and 2 demonstrated that visual heading estimates are indeed affected by the velocity profile of the movement trajectory, with lower thresholds observed for the R-Vis compared to the C-Vis. In Exp. 2 when visual–vestibular inputs were both present, they were combined in a statistically optimal fashion irrespective of the type of visual velocity profile, thus demonstrating robust integration of visual and vestibular cues. The study suggests that while the time course of the velocity did affect visual heading judgments, a moderate conflict between visual and vestibular motion profiles does not cause a breakdown in optimal integration for heading.

A1 J. S. Butler · J. L. Campos · H. H. Bühlhoff (✉)
A2 Max Planck Institute for Biological Cybernetics,
A3 Spemanstrasse 38, 72076 Tübingen, Germany
A4 e-mail: heinrich.buelthoff@tuebingen.mpg.de

A5 J. S. Butler (✉)
A6 Trinity Centre for Bioengineering, Trinity College Dublin,
A7 Dublin 2, Ireland
A8 e-mail: jsbutler@gmail.com

A9 J. L. Campos
A10 iDAPT, Toronto Rehabilitation Institute, UHN, Toronto, Canada

A11 J. L. Campos
A12 Department of Psychology, University of Toronto,
A13 Toronto, Canada

A14 H. H. Bühlhoff
A15 Department of Brain and Cognitive Engineering,
A16 Korea University, Seoul, South Korea

Keywords Multisensory integration · Self-motion ·
Maximum likelihood estimation · Optimal integration ·
Acceleration · Visual · Vestibular

59 Introduction

AQ2 As a car travels down 5th Avenue in New York, it accelerates and decelerates every 100 m in response to the traffic signals, while avoiding vehicle and pedestrian traffic and staying within the lane. In order to achieve this successfully, several movement parameters must be effectively perceived, including heading direction and velocity. These movement parameters are perceived using multiple sensory systems, including the visual and vestibular systems. Previous research has shown that both heading (Warren and Hannon 1988; Royden et al. 1992, 1994; Butler et al. 2010; Fetsch et al. 2010a) and relative ego-velocity (Gibson 1950; Frenz and Lappe 2005) can be perceived using visual information alone in the absence of physical cues to motion. In contrast, while there has been a great deal of research assessing the capacity to visually judge the accelerations of external objects (e.g., Brouwer et al. 2002; Schlack and Albright 2007; Schlack et al. 2007, 2008), far fewer studies have considered the capacity of humans to judge accelerations/decelerations in the context of self-motion. Festl et al. (2012) have shown that humans can extract information from optic flow in order to discriminate motion profiles specifying different rates of acceleration. However, this study also concluded that absolute judgments of ego-accelerations are not possible without visual scaling of the scene provided through depth cues (and/or without the scaling provided through non-visual cues).

In terms of vestibular contributions to self-motion perception, a collection of recent research by our group and others has shown that vestibular information alone can also be used to perceive heading in humans and non-human primates (Telford et al. 1995; Butler et al. 2006; de Winkel et al. 2010; Fetsch et al. 2010a; MacNeilage et al. 2010; Crane 2012; Nolan et al. 2012; Cuturi and MacNeilage 2013). During translational motion, the main function of the vestibular system is as an acceleration detector. As the vestibular system responds to changes in acceleration, it cannot directly estimate velocity and therefore becomes uninformative during constant velocity motion (Benson et al. 1986).

Recent inquires have now begun to focus on how information from the visual and vestibular systems are integrated to perceive different aspects of self-motion. Because each of these sensory systems have different reliabilities for perceiving different movement parameters (i.e., vision more sensitive to changes in position and velocity and vestibular more sensitive to detecting accelerations) and for different movement conditions (e.g., vision more sensitive for slow and vestibular more sensitive for fast ego-motion (Berthoz et al. 1975; Zacharias and Young 1981)), thus the optimal combination of the cues should take into account the reliability of the single cue percepts. Indeed, within the

context of heading perception, behavioral and neurophysiological studies have shown that when visual and vestibular cues are presented synchronously, they elicit a more reliable behavioral and neuronal response than either cue alone (Butler et al. 2010, 2011a; Fetsch et al. 2010a, 2012; Gu et al. 2011). These results have been embedded into the theoretical framework of maximum likelihood estimation (MLE), such that predictions about the reliability and the weights of the unisensory cues can be used to make predictions in combined cue conditions (see Ernst and Banks 2002; Ernst and Bühlhoff 2004). Neurophysiological recordings in non-human primates have revealed heading direction sensitive neurons in areas such as MT, medial superior temporal (MST) and ventral intraparietal (VIP). Models of this neurophysiological data have indicated that vestibular responses are driven mainly by velocity (VIP and MSTd) and acceleration (VIP) components, whereas visual responses were driven mainly by velocity (VIP) (Fetsch et al. 2010b; Chen et al. 2011).

Far fewer studies have attempted to quantify the relative contributions of visual and vestibular cues to the perception of linear acceleration (Berger and Bühlhoff 2009; Berger et al. 2010). Berger et al. (2010) asked observers to judge how “believable” a forward accelerating movement was under different visual–vestibular conditions. Their results indicated that a simulated visual acceleration that coincided with a physical backward pitch was rated as most believable. However, the range of physical pitch movements that were rated as believable when combined with the same visual acceleration profile was quite broad. Further, the reasonably high tolerance for physical motions that differed from the visual motions did not seem to be affected by whether the observer was consciously aware of the discrepancy, indicating that this integration is likely quite robust.

There remains a gap in knowledge within this field of research regarding how different spatiotemporal characteristics of a self-motion profile, including information about heading and velocity interact. Given that self-motion perception is not well represented by a discrete event, but takes place over space and time, it is likely that there is a continuous integration of information throughout a given trajectory. This integration may therefore be dependent on different dynamic spatiotemporal parameters and may be contingent on individual sensory cue reliabilities. For instance, it is not yet clear whether the precision of heading perception could be affected by the velocity profile of the motion trajectory. It is also not clear whether the process by which visual and vestibular cues are integrated is affected by whether the visual and vestibular motion profiles are different.

Therefore, in order to first evaluate whether the velocity profile of a motion trajectory affects heading

164 perception, Experiment 1 evaluated heading discrimi-
 165 nation performance on a purely visual heading task for
 166 different velocity profile conditions. Specifically, head-
 167 ing comparisons were made for either constant velocity
 168 motion profiles or raised cosine velocity profiles. If visual
 169 heading discrimination thresholds are purely based upon
 170 displacement, there should be no performance differences
 171 between the two visual motion conditions. As velocity
 172 is the first derivative of displacement, it is impossible
 AQ3 to change one without changing the other. Therefore, in
 174 order to create discrepancies in velocities between the two
 175 motion profiles (visual and vestibular), while keeping dis-
 176 placement equal (important to control for in the context of
 177 heading perception), average velocity was equated across
 178 profiles.”

179 In contrast, if higher derivatives (acceleration) do play
 180 a role in visual heading perception, this could lead to sev-
 181 eral different predictions. First, given that a raised cosine
 182 velocity profile is the more natural and commonly experi-
 183 enced visual motion profile and is typically coincident
 184 with actual physical self-motion, it is possible that the dis-
 185 crimination thresholds will in fact be lower in the raised
 186 cosine velocity trials compared to the constant velocity
 187 trials. Another reason why the raised cosine velocity tri-
 188 als might result in a more reliable response is that partic-
 189 ipants may not integrate information across the whole
 190 profile but rather over a shorter window of time than the
 191 one second trials which could result in a higher velocity
 192 and hence a more reliable heading percept (Crowell and
 193 Banks 1993).

194 However, when considering the visual alone condi-
 195 tions, the vestibular cue is indicating no changes in veloc-
 196 ity which could introduce an intersensory conflict. This
 197 conflict may be greater for the raised cosine visual motion
 198 profile given as there is a change in velocity which is in
 199 conflict with the vestibular cue which might result in a less
 200 reliable discrimination of heading.

201 Experiment 2 helped to further test the role of the visual
 202 motion profile on self-motion by assessing multisensory
 203 heading perception when visual and vestibular cues were
 204 combined. Specifically, this experiment evaluated whether
 205 visual and vestibular cues would be optimally combined,
 206 even when the motion profiles of each differ. Again, the
 207 same two visual motion profiles were included during
 208 multisensory conditions, leading to cue combinations that
 209 were either congruent (both raised cosine velocity profiles)
 210 or incongruent (constant velocity visual motion and raised
 211 cosine velocity vestibular motion). This also allowed us to
 212 evaluate whether visual and vestibular inputs continued to
 213 be optimally integrated during self-motion (as has already
 214 be shown several times previously using this paradigm)
 215 when the visual velocity profile and the physical/vestibular
 216 velocity profile are discrepant.

Methods

Participants

15 Fifteen participants (five males) completed Experiment 1,
 16 and six new participants (two males) completed Experi-
 17 ment 2. The average age was 24 years (19–31). All partici-
 18 pants had normal or corrected-to-normal vision, including
 19 normal stereo vision. Participants were compensated with
 20 pay of 8 Euros per hour and were naïve to the purposes of
 21 the experiment. Participants gave their informed consent
 22 before taking part in the experiment, which was performed
 23 in accordance with the ethical standards specified in the
 24 1964 Declaration of Helsinki.

Apparatus

Experiment 1

231 In Experiment 1, participants were seated 1.0 m in front
 232 of a large back-projected screen. The screen had a field of
 233 view of $102^\circ \times 82^\circ$ with a resolution of $1,280 \times 1,024$ pix-
 234 els and a refresh rate of 60 frames per second.

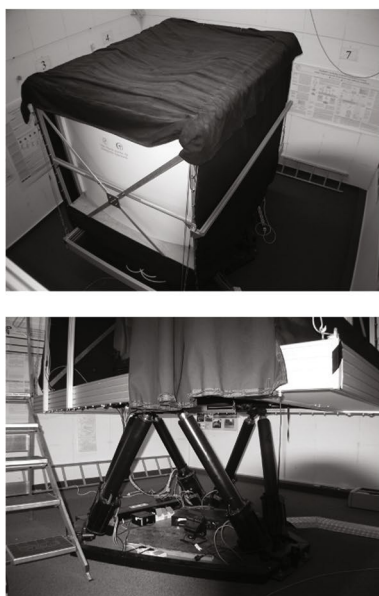
Experiment 2

236 The experimental setup and stimuli were identical to those
 237 described previously (Butler et al. 2010, 2011a). This
 238 experiment was conducted in the Motion Lab at the Max
 239 Planck Institute for Biological Cybernetics, which consists
 240 of a Maxcue 600, six degree of freedom, Stewart platform
 241 manufactured by Motion-Base PLC, UK (Fig. 1a).

242 To mask the noise of the platform, participants wore
 243 noise-cancellation headphones with two-way communica-
 244 tion capability while white noise was played. To mask the
 245 vibrations of the platform motors, somatosensory vibra-
 246 tions were produced by subwoofers installed under the seat
 247 and foot plate. A foam head rest was used to keep head
 248 movements to a minimum. The visuals were displayed on
 249 a projection screen with a field of view of $86^\circ \times 65^\circ$ and
 250 a resolution of 1400×1050 pixels and a refresh rate of
 251 60 frames per second. Participants viewed the projection
 252 screen through an aperture, which reduced the field of view
 253 to $50^\circ \times 50^\circ$, thereby increasing immersion and avoiding
 254 conflicting information provided by the stability of the
 255 frame around the screen and the visual motion information
 256 being projected on the screen. In both experiments, partici-
 257 pants freely viewed the stimulus.

258 Participants responded using a four-button response
 259 box. The stereoscopic image was generated using red–cyan
 260 anaglyphs. All experiments were coded using a graphical
 261 real-time interactive programming language (Virtools™,
 262 France).

(A) Hexapod Platform



(B) Motion Profiles

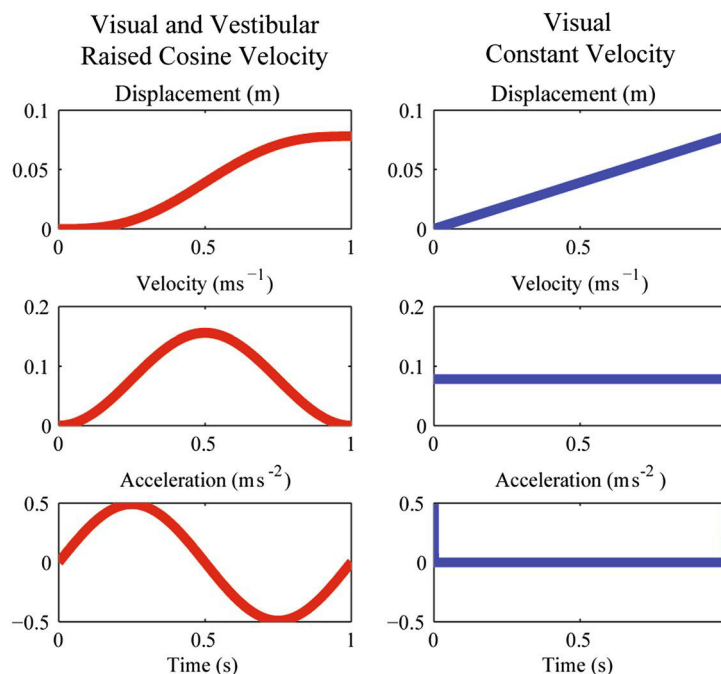


Fig. 1 **a** Top view of the hexapod platform. Bottom view of the hexapod platform, **b** displacement, velocity and acceleration of the motion profiles. Left, raised cosine velocity profile for the vestibular and vis-

ual conditions (red). Right, constant velocity profile which is only for the visual condition (blue)

263 Stimuli

264 The visual stimulus in both Experiments 1 and 2 consisted of a limited lifetime Gaussian starfield. Each star was a circle that had an average diameter of 0.15° which were Gaussian smoothed in contrast to minimize any sharp contrast changes and hence avoid aliasing and a lifetime in the range of 0.5–1.0 s. The maximum number of stars on the screen at one time was 200, and the minimum was 150. Each dot subtended between 0.1° and 0.2° , which depended on their virtual distance ranging from 2 to 2.5 m. The starfield was presented in stereo on a gray background to facilitate the fusing of the red and cyan images.

275 Two motion profiles were used in this study, a raised cosine velocity profile (acceleration/decelerations at start/end of motion) and a constant velocity profile (step function with a single impulse in acceleration at the start and of the motion). If visual heading discrimination thresholds are purely based upon displacement, there should be no performance differences between the two visual motion conditions. The raised cosine velocity profile was

$$283 \quad s_{\text{Raised}}(t) = 0.49 \frac{(2\pi t - \sin(2\pi t))}{4\pi^2}, \quad 0 \leq t \leq 1s. \quad (1)$$

284 This profile had a maximum displacement, velocity and acceleration of 0.078 m, 0.156 ms^{-1} and 0.49 ms^{-2} ,

286 respectively (Fig. 1b Left), which is above the detection threshold for blindfolded accelerations (Benson et al. 1986).

287 The constant velocity profile, which was only employed in the visual condition, was

$$289 \quad s_{\text{constant}}(t) = 0.078t, \quad 0 \leq t \leq 1s. \quad (2)$$

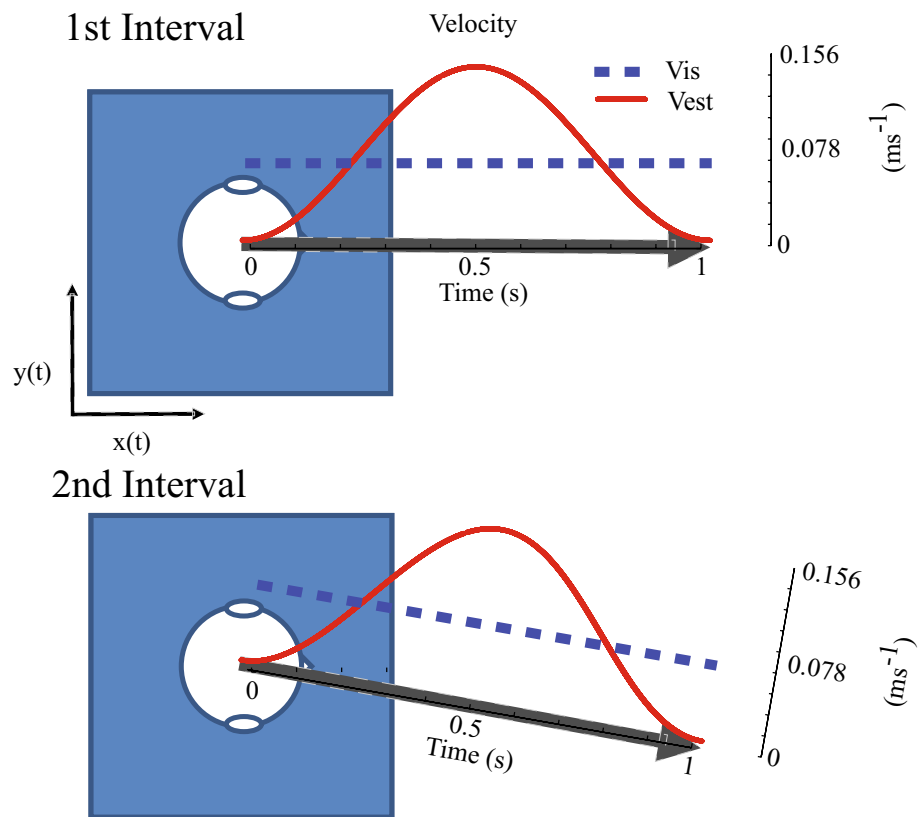
292 This profile has a maximum displacement and velocity of 0.078 m and 0.078 ms^{-1} , respectively. The acceleration profile is 0.0 ms^{-2} except for an impulse at the very start and end of the profile (Fig. 1b Right).

296 General procedure

297 Participants performed a two-interval forced choice task (2-IFC) in which they were asked to judge “in which of the two intervals did you move more to the right” (see Fig. 2). Each trial consisted of two heading motions, the standard and the comparison (counterbalanced across trials). The standard angle was always fixed at 0° (straight ahead), while the eight comparison angles were $-20^\circ -10^\circ -5^\circ -2^\circ, 2^\circ 5^\circ, 10^\circ$ and 20° . All trials were initiated with a beep to indicate that the participants could start the trial with a button press. After pressing the start button, there was a 0.75-s pause between the stimulus appearing on the screen and the onset of the motion. Between intervals, there



Fig. 2 Top-down schematic of a 2-IFC combined incongruent trial, in which the motion profile for the visual cue is a constant velocity (blue) and the vestibular cue is a raised cosine (red)



309 was a 1-s pause. Participants responded after the second
 310 interval. In the vestibular and visual–vestibular conditions
 311 in Experiment 2, after responding, the participants were
 312 passively moved back to the start position with no visual
 313 stimulus on the screen at a subthreshold vestibular velocity
 314 of 0.025 ms^{-1} , for about 5 s prior to commencing the next
 315 trial.

316 Experiment 1

317 Participants completed a visual alone heading task. The
 318 heading task was blocked with respect to the different
 319 motion profiles, a constant velocity profile (C-Vis) and a
 320 raised cosine velocity profile (R-Vis), which were coun-
 321 terbalanced across participants. For each condition, there
 322 were 30 repetitions of each of the eight comparison angles
 323 (240 trials total). These trials were divided into three blocks
 324 with each block lasting approximately 7 min. In total with
 325 breaks, the experiment lasted 1 h.

326 Experiment 2

327 Six naïve participants completed six blocks of visual alone
 328 trials (3 C-Vis, 3 R-Vis), three blocks of vestibular alone
 329 trials and six blocks of visual–vestibular trials (3 C-Vis/
 330 Vest, 3 R-Vis/Vest). Therefore, in the combined cue trials
 331 (visual–vestibular), half were congruent (R-Vis/R-Vest),

and half were incongruent (C-Vis/R-Vest) (see Fig. 2).
 Each block consisted of eight comparison angles repeated
 ten times (240 trials per condition). The experiment was
 run over five one and a half hour experimental sessions.

Data analysis

Individual participant's data for each condition were fit
 with a Gaussian psychometric function using the psignifit
 toolbox (Wichmann and Hill 2001a, b). From the calculated
 fit, the just noticeable differences (JNDs) were determined,
 which is proportional to the standard deviation of the dis-
 tribution. The JND value is inversely related to reliability,
 and thus, the higher the JND, the higher the discrimination
 threshold and the lower the reliability. For all analyses, the
 significance level was set at 0.05.

Results

Experiment 1

Figure 3a shows data from a representative partici-
 pant for the visual alone raised cosine velocity condi-
 tion (red) and visual alone constant velocity condition
 (blue) and cumulative Gaussian fits. The average visual
 alone heading thresholds for the R-Vis and C-Vis were

Visual Conditions

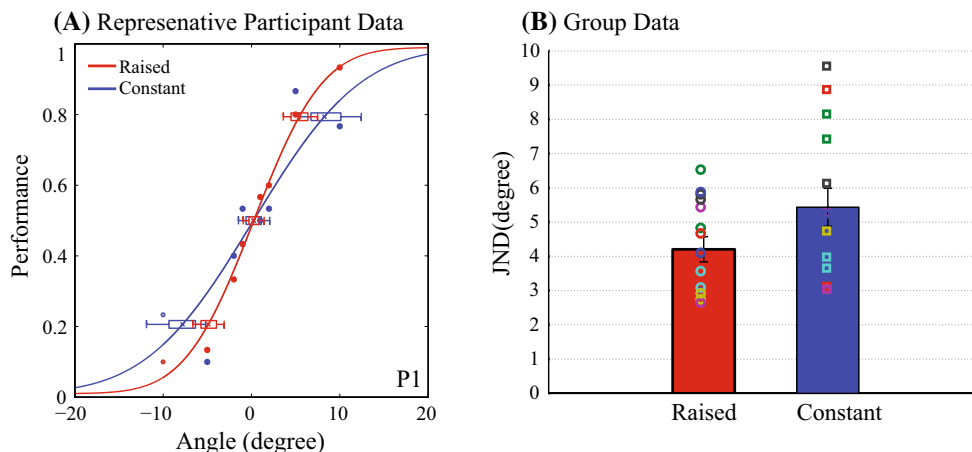


Fig. 3 Experiment 1 results. **a** Data for raised cosine visual alone (red), constant visual alone (blue) and for a representative participant. The data show the proportion of perceived “more rightward” responses as a function of heading angle. Solid lines represent the cumulative Gaussian functions that were fitted to the data. Box plots

whiskers indicate the bootstrapped confidence intervals at -2 , -1 , 1 and 2 standard deviations. **b** Visual alone group average heading JNDs for the different motion profiles. Error bars represent standard error of the mean. Open circles/squares represent individual participants

353 $JND_{R-Vis} = 4.20^\circ \pm 0.37^\circ$ and $JND_{C-Vis} = 5.43^\circ \pm 0.55^\circ$,
 354 respectively (Fig. 3b). The results of a paired two-tailed
 355 t test revealed that the JNDs for the R-Vis condition were
 356 significantly lower than the C-Vis condition ($t_{15} = -3.298$;
 357 $p < 0.005$). These results indicate that the type of motion
 358 profile affects the discrimination of heading. Furthermore,
 359 the more natural yet complex visual motion profile (R-Vis)
 360 yielded the most reliable responses.

361 Experiment 2

362 Based on MLE models and supported by past studies, a
 363 combination of congruent visual and vestibular inputs
 364 should result in a reduction of variance compared to unisen-
 365 sory conditions (Fetsch et al. 2009, 2010a; Butler et al.
 366 2010, 2011a). What is unknown is whether optimal integra-
 367 tion will occur if there is conflicting information provided
 368 by the visual and vestibular inputs in the form of different
 369 velocity profiles and how these results compare to visual
 370 only conditions. If the combined visual and vestibular cues
 371 are integrated irrespective of whether the motion profiles
 372 are congruent or incongruent, the unimodal JNDs, JND_{Vis} ,
 373 JND_{Vest} , can be used to predict the optimal JND_{Pred} of the
 374 visual–vestibular condition (Ernst and Bühlhoff 2004).

$$375 \quad JND_{Pred\ Vis-Vest}^2 = \frac{1}{1/JND_{Vis}^2 + 1/JND_{Vest}^2} = \frac{JND_{Vis}^2 JND_{Vest}^2}{JND_{Vis}^2 + JND_{Vest}^2} \quad (3)$$

376 If the cues are not optimally combined, as has been the
 377 case in some previous studies under certain conditions (de
 378 Winkel et al. 2010; Butler et al. 2011a), then the JND in the

combined conditions would be no less than the JND of the
 most reliable unimodal cue.

$$JND_{Vis-Vest} \geq \min(JND_{Vis}, JND_{Vest}) \quad (4)$$

The 95 % confidence intervals were calculated for each
 participant’s JND by a bootstrap procedure with 1999 rep-
 etitions (for details see Wichmann and Hill 2001b). The
 predicted multisensory 95 % confidence intervals Δ_{Pred}
 were calculated by the propagation of error formula (Taylor
 1997)

$$\Delta_{Pred} = \left| \frac{\partial JND_{Vis-Vest}}{\partial JND_{Vis}} \right| \Delta_{Vis} + \left| \frac{\partial JND_{Vis-Vest}}{\partial JND_{Vest}} \right| \Delta_{Vest} \quad (5)$$

from the first derivatives of the predicted visual–vestibular
 JND_{Pred} and the visual Δ_{Vis} and vestibular Δ_{Vest} confi-
 dence intervals.

Unimodal conditions

The average visual alone heading JNDs for the R-Vis and
 C-Vis were $JND_{R-Vis} = 5.5^\circ \pm 0.54^\circ$, $JND_{C-Vis} = 7.3^\circ \pm$
 0.83° , thereby replicating the results of Experiment 1 with a
 different group of participants. This also demonstrates that
 even though there were differences in the visual displays
 in Experiments 1 and 2, including different FOVs and an
 aperture, the result that the velocity profile had an impact
 on the reliability of the visual alone heading response was
 unchanged. For vestibular alone heading, the JND_{Vest} was
 $5.6^\circ \pm 0.76^\circ$ (Fig. 4a). An ANOVA was performed on the
 heading discrimination performance (JND) for the R-Vis



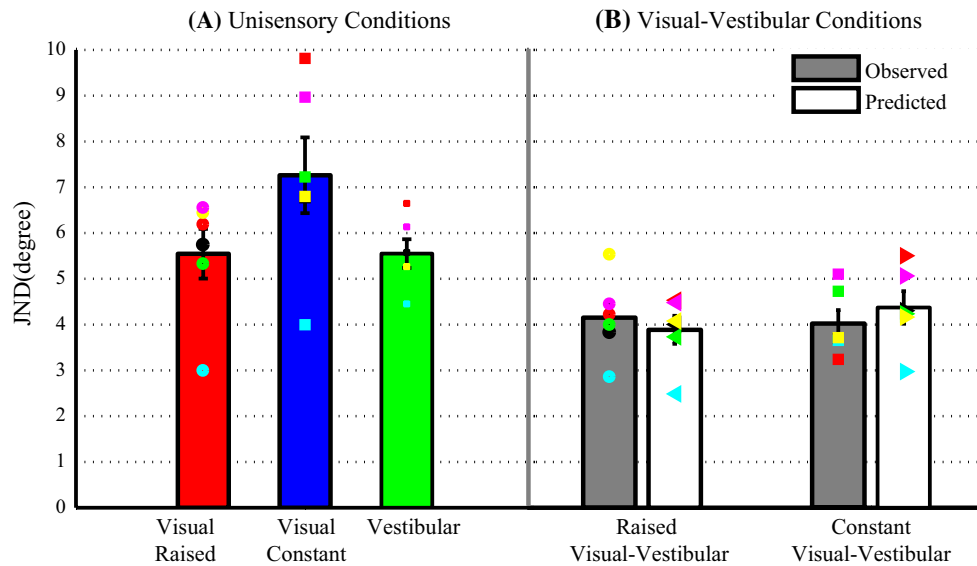


Fig. 4 Experiment 2 results. **a** Unimodal average heading JNDs. **b** Bimodal observed and predicted average heading JNDs for the congruent and incongruent motion profile conditions. *Error bars*

represent standard error of the mean. *Overlaid symbols* represent individual participants for each condition

404 alone, C-Vis alone and Vest alone for all participants. The
 405 analysis revealed a significant main effect of condition
 406 ($F(2, 10) = 9.086$, $MSE = 0.646$, $p < 0.01$). Three two-
 407 tailed paired-sample t tests were conducted to compare the
 408 unimodal conditions, R-Vis vs. C-Vis, R-Vis vs. Vest and
 409 C-Vis vs. Vest. As in Experiment 1, the R-Vis and C-Vis
 410 alone were significantly different ($t_5 = -3.552$, $p < 0.016$).
 411 The C-Vis condition was significantly different from the
 412 Vest alone condition (C-Vis: $t_5 = -3.22$, $p < 0.025$), but the
 413 R-Vis was not significantly different from the Vest alone
 414 condition ($p = 0.993$).

415 **Bimodal conditions**

416 The observed and predicted average JNDs for the bimodal
 417 congruent motion profiles were $JND_{Obs_R-Vis/R-Vest} =$
 418 $4.15^\circ \pm 0.35^\circ$, and $JND_{Pred_R-Vis/R-Vest} = 3.88^\circ \pm 0.31^\circ$,
 419 respectively. The observed and predicted average
 420 JNDs for the bimodal incongruent motion profile were
 421 $JND_{Obs_C-Vis/R-Vest} = 4.03^\circ \pm 0.29^\circ$, $JND_{Pred_C-Vis/R-Vest}$
 422 $= 4.37^\circ \pm 0.35^\circ$ (Fig. 4b), respectively.

423 To compare the multisensory conditions with the visual
 424 conditions and the role of motion profile, the data were sub-
 425 mitted to a 2 sensory condition (Vis alone vs. Vis–Vest) \times 2
 426 motion profile (C-Vis vs. R-Vis) repeated measures
 427 ANOVA. The analysis showed a significant effect of sensory
 428 condition ($F(1,5) = 18.115$, $MSE = 1.779$, $p < 0.01$),
 429 but no significant effect of motion profile ($F(1,5) = 3.768$,
 430 $MSE = 0.710$, $p = 0.069$) and a significant interaction

effect ($F(1,5) = 5.105$, $MSE = 0.567$, $p = 0.03$). The sig-
 431 nificant interaction is driven by the statistical difference
 432 between the profiles in the visual conditions (see above) but
 433 not for the combined condition (Post hoc t test: C-Vis–Vest
 434 vs. R-Vis–Vest: $t_5 = 0.296$, $p = 0.776$).
 435

436 Follow-up paired-sample t tests to investigate the effect
 437 of sensory condition revealed a lower JND in the Vis–
 438 Vest condition than the Visual Alone for both the raised
 439 cosine and constant velocity profile (R-Vis vs. R-Vis–Vest:
 440 $t_5 = 3.917$, $p < 0.015$ and C-Vis vs. C-Vis–Vest: $t_5 = 4.463$,
 441 $p < 0.01$). To compare the multisensory conditions with
 442 the vestibular alone condition, the vestibular JND was sub-
 443 mitted to a paired t tests with the raised Vis–Vest JND and
 444 the constant Vis–Vest JND which revealed a lower JND in
 445 the Vis–Vest conditions (Vest vs. R-Vis–Vest: $t_5 = 3.808$,
 446 $p < 0.015$ and Vest vs. C-Vis–Vest: $t_5 = 3.34$, $p < 0.025$).
 447 This shows that there was increased reliability of the head-
 448 ing response in the visual–vestibular condition for both the
 449 congruent and incongruent conditions.

450 In order to compare the observed results with model
 451 predictions (based on MLE optimal integration), a 2
 452 (observed vs. predicted) \times 2 motion profile (C-Vis vs.
 453 R-Vis) repeated measures ANOVA was performed. The
 454 analysis revealed that observed and predicted JNDs were
 455 not significantly different ($F(1,5) = 0.494$, $MSE = 0.022$,
 456 $p = 0.89$), nor was there a main effect of motion profile
 457 ($F(1,5) = 0.0556$, $MSE = 0.346$, $p = 0.49$) or an interac-
 458 tion effect ($F(1,5) = 2.085$, $MSE = 0.275$, $p = 0.21$). The
 459 results show that for both the congruent condition (R-Vis/
 460 R-Vest) and the incongruent condition (C-Vis/R-Vest), an

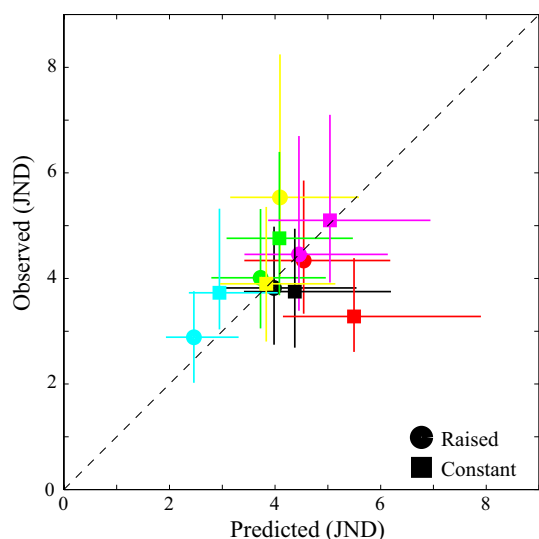


Fig. 5 Scatterplot of predicted visual-vestibular JNDs versus observed visual-vestibular JNDs. Different symbols represent different visual motion profiles (circles = R-Vis/R-Vest and squares = C-Vis/R-Vest). Different colors represent individual participants. The dashed line indicates the ideal data. Error bars represent 95 % bootstrapped confidence intervals

461 optimal reduction in variance was observed that was in line
462 with MLE model predictions (Fig. 5).

463 Discussion

464 The results of both Experiment 1 and 2 demonstrate that
465 visual velocity motion profiles can affect visual heading
466 discrimination. The most typical and natural form of visual
467 motion that occurs when changing from a stationary to a
468 moving position includes an initial acceleration component
469 followed by a deceleration component prior to the final
470 resting state. Indeed, the current results show that it is this
471 type of profile that resulted in the least variable visual heading
472 estimates. In contrast, when the visual motion started
473 suddenly (constant velocity), which is an event that does
474 not typically occur during real world interactions, higher
475 thresholds were observed. This suggests that despite the
476 fact that the instructed task at hand (heading perception)
477 was mainly contingent on detecting changes in direction,
478 other spatial-temporal features of the motion profile (i.e.,
479 velocity/acceleration in this case) affected the sensitivity
480 of responding. It is not entirely clear based on these initial
481 findings what the nature of this relationship is. It is possible,
482 for instance, that having a natural acceleration component
483 to the visual motion helps to disambiguate self-motion
484 from object motion (Festl et al. 2012). It is also possible
485 that having an acceleration component to the visual motion
486 generates a more compelling sense of “vection” or illusory

self-motion, which could improve measures of self-motion
perception. Indeed, there are many examples demonstrating
that ratings of vection are higher when acceleration
components are added to a purely visual motion stimulus
(e.g., viewpoint jitter) compared to when constant velocity
visual motion is presented (Palmisano et al. 2000, 2003,
2007, 2008, 2011). Notably, vection onsets typically occur
after longer periods of constant velocity than was afforded
by the stimulus duration used here. This is presumably
because illusory visual motion becomes most compelling
once the conflicting expectation of the vestibular onset
cue to motion (i.e., the acceleration component) subsides
(Palmisano et al. 2008). However, the current results demonstrate
that even within the 1-s stimulus presented here, significant
differences in the sensitivity to visual acceleration profiles
are clearly observed.

It should also be noted that the depth scaling information
provided by the starfield stimuli that was used in the current
study was only provided through stereo cues, and therefore,
estimates of absolute velocity/acceleration were not possible
(relative comparisons only). It is conceivable that having
scaling information from richer depth cues may also impact
the extent to which visual velocity profiles affect heading
discrimination.

The second main finding of this study was that when
the different visual velocity motion profiles were presented
simultaneously with vestibular inputs, optimal cue integration
was observed irrespective of whether the cues were congruent
(R-Vis and R-Vest) or incongruent (C-Vis and R-Vest).
This suggests that the integration of visual and vestibular
cues is quite robust and tolerant of spatiotemporal conflicts.
In the context of multisensory integration for other sensory
combinations (e.g., visual-tactile, visual-auditory), a
wealth of evidence has shown that optimal integration is
affected by cue coincidence in space and/or time
(Hartcher-O’Brien et al. 2014). That is, when information
from two sensory systems occur at locations that are too far
apart or occur at moments that are too far separated in
time, these inputs are not perceived as being associated
with one event and thus optimal integration fails. Specifically,
this can lead to the reliability of the responses under
multisensory conditions being equal to or worse than either
of the unisensory conditions (Wallace et al. 2004; Gepshtein
et al. 2005; Roach et al. 2006; Kording et al. 2007; Bentzelzen
et al. 2009; Wozny et al. 2010; Wozny and Shams 2011).
It is worth noting that in our study while the temporal/
velocity profiles were incongruent, other characteristics
of the stimuli were consistent (e.g., the onset of the stimuli
and the heading information which were always congruent
across motion profiles). This could explain why participants
combined the visual and vestibular inputs in this case,
which is unlike other examples showing a breakdown of
optimal integration in the face of intersensory conflicts.



540 However, there are other recent examples that also dem- 593
 541 onstrate robust cue integration under conflicting sensory 594
 542 conditions. Raposo et al. (2012) and Sheppard et al. (2013) 595
 543 showed that both humans and rats combine audio and visual 596
 544 information over time in an optimal fashion even when the 597
 545 stimuli were not presented synchronously, thus illustrating 598
 546 that the time course of stimuli do not have to align in time 599
 547 for optimal integration. This result agrees with our findings 600
 548 such that even when the visual and vestibular motion pro- 601
 549 files are incongruent, participants combine the information 602
 550 in an optimal fashion. In a recent paper, Drugowitsch et al. 603
 551 (2014) have proposed a model of visual–vestibular integra- 604
 552 tion using a novel diffusion model in which visual veloc- 605
 553 ity information and vestibular acceleration information is 606
 554 accumulated over time to make a decision. This model does 607
 555 not require that the stimuli are synchronous but that the 608
 556 information for the decision is combined and accumulated 609
 557 over time. 610

558 The optimal integration of incongruent visual and ves- 611
 559 tibular motion profiles could be explained in relation to the 612
 560 brain acting as a moving average (low pass) filter of the 613
 561 sensory signals (Werkhoven et al. 1992). Thus, while the 614
 562 motion profiles are inconsistent at the start and the end of 615
 563 the movement, the period around the peak velocity could 616
 564 be perceived as similar and hence integrated. Furthermore, 617
 565 this could account for the more reliable visual alone head- 618
 566 ing responses in the raised cosine velocity profile condi- 619
 567 tion. While over the one second movement, the displace- 620
 568 ment and the average velocity are identical for both motion 621
 569 profiles if the heading discrimination judgment is made 622
 570 over a smaller window of time centered around the maxi- 623
 571 mum velocity than the raised cosine velocity profile would 624
 572 have a larger displacement and average velocity than the 625
 573 constant velocity profile and as higher velocities can result 626
 574 in a more accurate discrimination of heading (Crowell and 627
 575 Banks 1996). 628

576 Currently, very little is known about the tolerance of 629
 577 visual–vestibular integration to spatial or temporal con- 630
 578 flicts. There is evidence that visual–vestibular integration 631
 579 remains optimal under spatial discrepancies (Butler et al. 632
 580 2010; Fetsch et al. 2010b) and that the believability of for- 633
 581 ward accelerations is maintained under a range of physical 634
 582 pitch angles (MacNeilage et al. 2007; Berger et al. 2010). 635
 583 Ash and Palmisano (2012) have also demonstrated that 636
 584 vection is enhanced when visual and vestibular inputs are 637
 585 combined during oscillating head movements, even if the 638
 586 physical oscillations are not spatially congruent with the 639
 587 visual oscillations. In general, however, the range of motion 640
 588 parameters under which visual–vestibular conflicts lead to 641
 589 non-optimal integration is unknown. One possible limita- 642
 590 tion of this study is that we cannot speak to the relative 643
 591 weights of the visual and vestibular cues. Ideally, future 644
 592 research will sample from a wider and more comprehensive 645

range of spatial and temporal offsets, but it should be noted 593
 that in our previous work, there was a bias toward the ves- 594
 tibular cue which was not accounted for the by reliability 595
 of the cue which will have to be taken into consideration 596
 (Butler et al. 2010). 597

598 There is, however, reason to believe that the optimal 599
 600 integration of visual and vestibular inputs may be particu- 601
 602 larly resistant to cue conflicts, because unlike other cue 603
 604 combinations, these two cues maintain a very tight, causal 605
 relationship (MacNeilage et al. 2007; Frissen et al. 2011; 606
 Campos et al. 2012; Prsa et al. 2012). (Prsa et al. 2012) 607
 recently argued that mandatory fusion between visual and 608
 vestibular cues is observed during ego-rotations. Specifi- 609
 cally, they argue that unisensory estimates of rotations from 610
 visual and vestibular inputs are not retained once integra- 611
 tion has occurred. While mandatory fusion has been dem- 612
 onstrated for intramodal cue integration (e.g., visual cue 613
 integration—see Hillis et al. 2002), this is the first reported 614
 demonstration in the context of cross-modal integration. 615
 Future experiments would test the limit of the combination 616
 of the cues by including larger incongruencies between the 617
 visual and vestibular motion profiles. A caveat to the man- 618
 datory fusion argument is that multisensory integration can 619
 be stimulus and task specific; for example, auditory and 620
 tactile cues exhibit multisensory integration for frequency 621
 discrimination (Yau et al. 2009; Butler et al. 2012) but not 622
 for duration or intensity discrimination (Yau et al. 2010; 623
 Butler et al. 2011b). This could also be the case for visual– 624
 vestibular integration that for a different task mandatory 625
 integration might breakdown. 626

627 There are several applied implications for these find- 628
 629 ings in the context of both fixed-based and motion-based 629
 simulation (Teufel et al. 2007; Bles and Groen 2009; Bar- 630
 nnett-Cowan et al. 2012). For instance, it is not uncommon 631
 for purely visually based simulations (i.e., fixed-base) to 632
 refrain from using visual accelerations in an attempt to 633
 avoid the experiences of motion sickness that can be caused 634
 by sensory conflicts (Wallis et al. 2002). However, the use 635
 of such motion profiles could have more global effects on 636
 perception and performance across a variety of parameters 637
 (i.e., velocity and heading perception). In the context of 638
 motion-based simulators, it is typically the case that the 639
 range of movements being simulated extends beyond the 640
 motion capabilities of the platform, and therefore, motion 641
 cueing algorithms must be used to create the illusion of 642
 extended motion (Grant and Reid 1997). One of the key 643
 necessities of these algorithms is to ensure an acceptable 644
 congruency between visual and physical motion cues. The 645
 results of the current study suggest that the inclusion of 646
 physical motion leads to more precise estimates of self- 647
 motion and that this precision persists even when conflicts 648
 are present between visual and physical inputs. Under- 649
 standing the range of tolerable conflicts will help to better 650

646 define motion cueing algorithms in future and maximize
647 the capabilities of such simulations.

648 Conclusion

649 The study demonstrates that, while visual velocity profiles
650 can affect the sensitivity of visual heading discrimination, a
651 conflict between visual and vestibular velocity profiles does
652 not cause a breakdown in optimal integration for heading.
653 This suggests that optimal visual–vestibular integration
654 is robust in the face of some spatiotemporal conflicts and
655 future work will help to define the extent to which these
656 types of conflicts are tolerated before integration breaks
657 down.

658 **Acknowledgments** This research was supported by the Max
659 Planck Society and by the Brain Korea 21 PLUS Program through
660 the National Research Foundation of Korea funded by the Ministry
661 of Education. We are grateful to the participants for their time. We
662 are also grateful to Paul “Pogen” MacNeilage, Julian Hoffmann, Edel
663 Flynn, Karl Beykirch, Stuart Smith and Jack Loomis for their help at
664 different stages of this project.

665 References

666 Ash A, Palmisano S (2012) Vection during conflicting multisensory
667 information about the axis, magnitude, and direction of self-
668 motion. *Perception* 41:253–267
669 Barnett-Cowan M, Meilinger T, Vidal M, Teufel H, Bühlhoff HH
670 (2012) MPI CyberMotion Simulator: implementation of a novel
671 motion simulator to investigate multisensory path integration in
672 three dimensions. *J Vis Exp*. doi:10.3791/3436
673 Benson AJ, Spencer MB, Stott JR (1986) Thresholds for the detection
674 of the direction of whole-body, linear movement in the horizontal
675 plane. *Aviat Space Environ Med* 57:1088–1096
676 Bentvelzen A, Leung J, Alais D (2009) Discriminating audiovisual
677 speed: optimal integration of speed defaults to probability
678 summation when component reliabilities diverge. *Perception*
679 38:966–987
680 Berger DR, Bühlhoff HH (2009) The role of attention on the integra-
681 tion of visual and inertial cues. *Exp Brain Res* 198:287–300.
682 doi:10.1007/s00221-009-1767-8
683 Berger DR, Schulte-Pelkum J, Bühlhoff HH (2010) Simulating
684 believable forward accelerations on a Stewart motion plat-
685 form. *ACM transactions on applied perception* 7(Artn 5).
686 doi:10.1145/1658349.1658354
687 Berthoz A, Pavard B, Young LR (1975) Perception of linear horizon-
688 tal self-motion induced by peripheral vision (linearvection) basic
689 characteristics and visual–vestibular interactions. *Exp Brain Res*
690 23:471–489
691 Bles W, Groen E (2009) The DESDEMONA motion facility: applica-
692 tions for space research. *Microgravity Sci Technol* 21:281–286.
693 doi:10.1007/s12217-009-9120-1
694 Brouwer AM, Brenner E, Smeets JB (2002) Perception of accelera-
695 tion with short presentation times: can acceleration be used in
696 interception? *Percept Psychophys* 64:1160–1168
697 Butler JS, Smith ST, Beykirch K, Bühlhoff HH (2006) Visual vestib-
698 ular interactions for self motion estimation. In: Driving simulation
699 conference, Paris

700 Butler JS, Smith ST, Campos JL, Bühlhoff HH (2010) Bayesian inte-
701 gration of visual and vestibular signals for heading. *J Vis* 10:23.
702 doi:10.1167/10.11.23
703 Butler JS, Campos JL, Bühlhoff HH, Smith ST (2011a) The role of
704 stereo vision in visual–vestibular integration. *Seeing Perceiving*
24:453–470. doi:10.1163/187847511X588070
705 Butler JS, Molholm S, Fiebelkorn IC, Mercier MR, Schwartz TH,
706 Foxe JJ (2011b) Common or redundant neural circuits for dura-
707 tion processing across audition and touch. *J Neurosci* 31:3400–
708 3406. doi:10.1523/JNEUROSCI.3296-10.2011
709 Butler JS, Foxe JJ, Fiebelkorn IC, Mercier MR, Molholm S (2012)
710 Multisensory representation of frequency across audition and
711 touch: high density electrical mapping reveals early sensory-per-
712 ceptual coupling. *J Neurosci* 32:15338–15344. doi:10.1523/JNE-
713 UROSCI.1796-12.2012
714 Campos JL, Butler JS, Bühlhoff HH (2012) Multisensory integra-
715 tion in the estimation of walked distances. *Exp Brain Res*.
716 doi:10.1007/s00221-012-3048-1
717 Chen A, DeAngelis GC, Angelaki DE (2011) Representation of
718 vestibular and visual cues to self-motion in ventral intrapari-
719 etal cortex. *J Neurosci* 31:12036–12052. doi:10.1523/JNEURO-
720 SCI.0395-11.2011
721 Crane BT (2012) Direction specific biases in human visual and ves-
722 tibular heading perception. *PLoS One* 7:e51383. doi:10.1371/
723 journal.pone.0051383
724 Crowell JA, Banks MS (1993) Perceiving heading with differ-
725 ent retinal regions and types of optic flow. *Percept Psychophys*
726 53:325–337
727 Crowell JA, Banks MS (1996) Ideal observer for heading judgments.
728 *Vis Res* 36:471–490
729 Cuturi LF, MacNeilage PR (2013) Systematic biases in human
730 heading estimation. *PLoS One* 8:e56862. doi:10.1371/
731 journal.pone.0056862
732 de Winkel KN, Weesie J, Werkhoven PJ, Groen EL (2010) Integration
733 of visual and inertial cues in perceived heading of self-motion. *J*
734 *Vis* 10:1. doi:10.1167/10.12.1
735 Drugowitsch J, DeAngelis GC, Klier EM, Angelaki DE, Pouget A
736 (2014) Optimal multisensory decision-making in a reaction-time
737 task. *Elife*:e03005 doi: 10.7554/eLife.03005
738 Ernst MO, Banks MS (2002) Humans integrate visual and haptic
739 information in a statistically optimal fashion. *Nature* 415:429–
740 433. doi:10.1038/415429a
741 Ernst MO, Bühlhoff HH (2004) Merging the senses into a robust per-
742 cept. *Trends Cogn Sci* 8:162–169. doi:10.1016/j.tics.2004.02.002
743 Festl F, Reckenwald F, Yuan C, Mallot HA (2012) Detection of linear
744 ego-acceleration from optic flow. *J Vis* 12 doi: 10.1167/12.7.10
745 Fetsch CR, Turner AH, DeAngelis GC, Angelaki DE (2009) Dynamic
746 reweighting of visual and vestibular cues during self-motion
747 perception. *J Neurosci* 29:15601–15612. doi:10.1523/JNEURO-
748 SCI.2574-09.2009
749 Fetsch CR, Deangelis GC, Angelaki DE (2010a) Visual–vestibular
750 cue integration for heading perception: applications of opti-
751 mal cue integration theory. *Eur J Neurosci* 31:1721–1729.
752 doi:10.1111/j.1460-9568.2010.07207.x
753 Fetsch CR, Rajguru SM, Karunaratne A, Gu Y, Angelaki DE,
754 DeAngelis GC (2010b) Spatiotemporal properties of vestibular
755 responses in area MSTd. *J Neurophysiol* 104:1506–1522. doi:10.
756 1152/jn.91247.2008
757 Fetsch CR, Pouget A, DeAngelis GC, Angelaki DE (2012) Neural
758 correlates of reliability-based cue weighting during multisensory
759 integration. *Nat Neurosci* 15:146–154. doi:10.1038/nn.2983
760 Frenz H, Lappe M (2005) Absolute travel distance from optic flow.
761 *Vis Res* 45:1679–1692. doi:10.1016/j.visres.2004.12.019
762 Frissen I, Campos JL, Souman JL, Ernst MO (2011) Integration of
763 vestibular and proprioceptive signals for spatial updating. *Exp*
764 *Brain Res* 212:163–176. doi:10.1007/s00221-011-2717-9
765



- 766 Gepshtein S, Burge J, Ernst MO, Banks MS (2005) The combination
767 of vision and touch depends on spatial proximity. *J Vis* 5:1013–
768 1023. doi:[10.1167/5.11.7](https://doi.org/10.1167/5.11.7)
- 769 Gibson JJ (1950) *The perception of the visual world*. Houghton
770 Mifflin, Boston
- 771 Grant PR, Reid LD (1997) Motion washout filter tuning : rules and
772 requirements. *American Institute of Aeronautics and Astronautics*,
773 Reston
- 774 Gu Y, Liu S, Fetsch CR et al (2011) Perceptual learning reduces
775 interneuronal correlations in macaque visual cortex. *Neuron*
776 71:750–761. doi:[10.1016/j.neuron.2011.06.015](https://doi.org/10.1016/j.neuron.2011.06.015)
- 777 Hartcher-O'Brien J, Di Luca M, Ernst MO (2014) The duration of
778 uncertain times: audiovisual information about intervals is inte-
779 grated in a statistically optimal fashion. *PLoS One* 9:e89339.
780 doi:[10.1371/journal.pone.0089339](https://doi.org/10.1371/journal.pone.0089339)
- 781 Hillis JM, Ernst MO, Banks MS, Landy MS (2002) Combining sensory
782 information: mandatory fusion within, but not between,
783 senses. *Science* 298:1627–1630. doi:[10.1126/science.1075396](https://doi.org/10.1126/science.1075396)
- 784 Kording KP, Beierholm U, Ma WJ, Quartz S, Tenenbaum JB, Shams
785 L (2007) Causal inference in multisensory perception. *PLoS One*
786 2:e943. doi:[10.1371/journal.pone.0000943](https://doi.org/10.1371/journal.pone.0000943)
- 787 MacNeilage PR, Banks MS, Berger DR, Bühlhoff HH (2007) A
788 Bayesian model of the disambiguation of gravito-inertial force
789 by visual cues. *Exp Brain Res* 179:263–290. doi:[10.1007/
790 s00221-006-0792-0](https://doi.org/10.1007/s00221-006-0792-0)
- 791 MacNeilage PR, Banks MS, DeAngelis GC, Angelaki DE (2010)
792 Vestibular heading discrimination and sensitivity to linear accel-
793 eration in head and world coordinates. *J Neurosci* 30:9084–9094.
794 doi:[10.1523/JNEUROSCI.1304-10.2010](https://doi.org/10.1523/JNEUROSCI.1304-10.2010)
- 795 Nolan H, Butler JS, Whelan R, Foxe JJ, Bühlhoff HH, Reilly RB
796 (2012) Neural correlates of oddball detection in self-motion
797 heading: a high-density event-related potential study of vestibular
798 integration. *Exp Brain Res*. doi:[10.1007/s00221-012-3059-y](https://doi.org/10.1007/s00221-012-3059-y)
- 799 Palmisano S, Gillam BJ, Blackburn SG (2000) Global-perspective jit-
800 ter improves vection in central vision. *Perception* 29:57–67
- 801 Palmisano S, Burke D, Allison RS (2003) Coherent perspective jitter
802 induces visual illusions of self-motion. *Perception* 32:97–110
- 803 Palmisano S, Bonato F, Bubka A, Folder J (2007) Vertical display
804 oscillation effects on forward vection and simulator sickness.
805 *Aviat Space Environ Med* 78:951–956
- 806 Palmisano S, Allison RS, Pekin F (2008) Accelerating self-motion
807 displays produce more compelling vection in depth. *Perception*
808 37:22–33
- 809 Palmisano S, Allison RS, Kim J, Bonato F (2011) Simulated view-
810 point jitter shakes sensory conflict accounts of vection. *Seeing*
811 *Perceiving* 24:173–200. doi:[10.1163/187847511X570817](https://doi.org/10.1163/187847511X570817)
- 812 Prsa M, Gale S, Blanke O (2012) Self-motion leads to mandatory cue
813 fusion across sensory modalities. *J Neurophysiol* 108:2282–2291.
814 doi:[10.1152/jn.00439.2012](https://doi.org/10.1152/jn.00439.2012)
- 815 Raposo D, Sheppard JP, Schrater PR, Churchland AK (2012) Multi-
816 sensory decision-making in rats and humans. *J Neurosci*
817 32:3726–3735. doi:[10.1523/JNEUROSCI.4998-11.2012](https://doi.org/10.1523/JNEUROSCI.4998-11.2012)
- 818 Roach NW, Heron J, McGraw PV (2006) Resolving multisensory
819 conflict: a strategy for balancing the costs and benefits of audio-
820 visual integration. *Proc Biol Sci* 273:2159–2168. doi:[10.1098/r
821 spb.2006.3578](https://doi.org/10.1098/rspb.2006.3578)
- Royden CS, Banks MS, Crowell JA (1992) The perception
822 of heading during eye movements. *Nature* 360:583–585.
823 doi:[10.1038/360583a0](https://doi.org/10.1038/360583a0)
- Royden CS, Crowell JA, Banks MS (1994) Estimating heading during
824 eye movements. *Vis Res* 34:3197–3214
825
- Schlack A, Albright TD (2007) Remembering visual motion: neural
826 correlates of associative plasticity and motion recall in cortical
827 area MT. *Neuron* 53:881–890. doi:[10.1016/j.neuron.2007.02.028](https://doi.org/10.1016/j.neuron.2007.02.028)
- Schlack A, Kregelberg B, Albright TD (2007) Recent history of stimu-
828 lus speeds affects the speed tuning of neurons in area MT. *J Neurosci*
829 27:11009–11018. doi:[10.1523/JNEUROSCI.3165-07.2007](https://doi.org/10.1523/JNEUROSCI.3165-07.2007)
- Schlack A, Kregelberg B, Albright TD (2008) Speed percep-
830 tion during acceleration and deceleration. *J Vis* 8(9):1–11.
831 doi:[10.1167/8.8.9](https://doi.org/10.1167/8.8.9)
- Sheppard JP, Raposo D, Churchland AK (2013) Dynamic weight-
832 ing of multisensory stimuli shapes decision-making in rats and
833 humans. *J Vis* 13 doi: [10.1167/13.6.4](https://doi.org/10.1167/13.6.4)
- Taylor JR (1997) *An introduction to error analysis : the study of*
834 *uncertainties in physical measurements*. University Science
835 Books, Sausalito
- Telford L, Howard IP, Ohmi M (1995) Heading judgments during
836 active and passive self-motion. *Exp Brain Res* 104:502–510
837
- Teufel H, Nusseck H-GG, Beykirch K, Butler JS, Kerger M, Bühlhoff
838 HH (2007) MPI motion simulator: development and analysis of a
839 novel motion simulator. In: *AIAA modeling and simulation tech-*
840 *nologies conference and exhibit*, South Carolina, pp 1–11
841
- Wallace MT, Roberson GE, Hairston WD, Stein BE, Vaughan
842 JW, Schirillo JA (2004) Unifying multisensory signals across
843 time and space. *Exp Brain Res* 158:252–258. doi:[10.1007/
844 s00221-004-1899-9](https://doi.org/10.1007/s00221-004-1899-9)
- Wallis G, Chatziastros A, Bühlhoff H (2002) An unexpected role for
845 visual feedback in vehicle steering control. *Curr Biol* 12:295–299
846
- Warren WH, Hannon DJ (1988) Direction of self-motion is perceived
847 from optical flow. *Nature* 336:162–163
848
- Werkhoven P, Snippe HP, Toet A (1992) Visual processing of optic
849 acceleration. *Vis Res* 32:2313–2329
850
- Wichmann FA, Hill NJ (2001a) The psychometric function: I. Fitting,
851 sampling, and goodness of fit. *Percept Psychophys* 63:1293–1313
852
- Wichmann FA, Hill NJ (2001b) The psychometric function: II. Boot-
853 strap-based confidence intervals and sampling. *Percept Psycho-*
854 *phys* 63:1314–1329
855
- Wozny DR, Shams L (2011) Recalibration of auditory space fol-
856 lowing milliseconds of cross-modal discrepancy. *J Neurosci*
857 31:4607–4612. doi:[10.1523/JNEUROSCI.6079-10.2011](https://doi.org/10.1523/JNEUROSCI.6079-10.2011)
- Wozny DR, Beierholm UR, Shams L (2010) Probability matching as
858 a computational strategy used in perception. *PLoS Comput Biol* 6
859 doi: [10.1371/journal.pcbi.1000871](https://doi.org/10.1371/journal.pcbi.1000871)
- Yau JM, Olenczak JB, Dammann JF, Bensmaia SJ (2009) Temporal
860 frequency channels are linked across audition and touch. *Curr*
861 *Biol* 19:561–566. doi:[10.1016/j.cub.2009.02.013](https://doi.org/10.1016/j.cub.2009.02.013)
- Yau JM, Weber AI, Bensmaia SJ (2010) Separate mechanisms for
862 audio-tactile pitch and loudness interactions. *Front Psychol*
863 1:160. doi:[10.3389/fpsyg.2010.00160](https://doi.org/10.3389/fpsyg.2010.00160)
- Zacharias GL, Young LR (1981) Influence of combined visual and
864 vestibular cues on human perception and control of horizontal
865 rotation. *Exp Brain Res* 41:159–171
866
867
868
869
870
871
872
873
874
875
876
877
878

Journal:	221
Article:	4136

Author Query Form

Please ensure you fill out your response to the queries raised below and return this form along with your corrections

Dear Author

During the process of typesetting your article, the following queries have arisen. Please check your typeset proof carefully against the queries listed below and mark the necessary changes either directly on the proof/online grid or in the 'Author's response' area provided below

Query	Details Required	Author's Response
AQ1	Please check and confirm inserted city name "Toronto" in the affiliation is correct .	
AQ2	Please confirm the section headings are correctly identified.	
AQ3	Please check for the missing quotes in the sentence 'Therefore, in order...equated across profiles'.	